

Nanoscale

Accepted Manuscript



This is an *Accepted Manuscript*, which has been through the Royal Society of Chemistry peer review process and has been accepted for publication.

Accepted Manuscripts are published online shortly after acceptance, before technical editing, formatting and proof reading. Using this free service, authors can make their results available to the community, in citable form, before we publish the edited article. We will replace this *Accepted Manuscript* with the edited and formatted *Advance Article* as soon as it is available.

You can find more information about *Accepted Manuscripts* in the [Information for Authors](#).

Please note that technical editing may introduce minor changes to the text and/or graphics, which may alter content. The journal's standard [Terms & Conditions](#) and the [Ethical guidelines](#) still apply. In no event shall the Royal Society of Chemistry be held responsible for any errors or omissions in this *Accepted Manuscript* or any consequences arising from the use of any information it contains.

Type-Tunable Amplified Spontaneous Emission from Core-Seeded CdSe/CdS Nanorods Controlled by Exciton-Exciton Interaction

Yusuf Kelestemur,^{‡,a} Ahmet Fatih Cihan,^{§,‡,a} Burak GuzelTURK^a and Hilmi Volkan Demir^{*.a,b}

*^aDepartment of Physics, Department of Electrical and Electronics Engineering,
UNAM – Institute of Materials Science and Nanotechnology, Bilkent University,
TR-06800, Ankara, Turkey*

*^bLuminous! Center of Excellence for Semiconductor Lighting and Displays, School of
Electrical and Electronic Engineering, School of Physical and Mathematical Sciences,
Nanyang Technological University, Nanyang Avenue, Singapore 639798, Singapore
E-mail: volkan@stanfordalumni.org*

Abstract

Type-tunable optical gain performance of core-seeded CdSe/CdS nanorods is studied via two-photon optical pumping. Controlling the exciton-exciton interaction by varying the core and shell size, blue-shifted, and red-shifted modes of amplified spontaneous emission are systematically and their type attributions are verified by time-resolved emission kinetics.

Colloidal semiconductor nanocrystals have recently arisen as promising candidates to be utilized as active gain media for lasing applications.^{1,2} With their band gap tunability (via size and shape modifications), efficient band edge emission (even at room temperature), discrete band structure, and synthesis through facile wet-chemistry, it is possible to achieve color-tunable, low-threshold, temperature insensitive and solution processed lasers from colloidal quantum dots (CQDs).²⁻⁶ However, there are various problems and challenges associated with CQD-based lasers. One way of achieving stimulated emission from the CQDs is through multi-exciton generation. When multiple excitons are formed, Auger recombination (AR) process becomes more pronounced and inhibits optical gain in CQDs.⁷⁻⁹ In addition, high intensity optical pumping, which is required for stimulated emission, can photo-damage the

sample and decrease the stability.¹⁰ To address these issues, CQDs having suppressed AR and exhibiting higher absorption cross-section, which can increase the stability of CQDs by lowering the optical gain threshold, are strongly required.

As a subclass of nanocrystals, core/shell nanorods (NRs) have been extensively considered for lasing applications and optical gain studies to overcome these problems with possibility of engineering their electronic structure for longer gain lifetime and increased absorption cross-section.¹¹⁻¹⁴ From different variety of core/shell NRs, core-seeded CdSe/CdS NRs have become quite attractive. With the advance in the colloidal synthesis of CdSe/CdS core/shell NRs, it is possible to synthesize highly efficient and crystalline CdSe/CdS core/shell NRs having a narrow size distribution by finely controlling their shape and size.^{15,16} Furthermore, due to shallow band offset for electrons in the CdSe/CdS core/shell material system, a partial separation of electron and hole wavefunctions is observed which is known as quasi Type-II electronic structure this contributes to the suppression of Auger recombination, which is highly critical for achieving lasing.^{11,16-18} The other advantage of having a lower energy barrier for electrons in CdSe/CdS NRs is that, by simply changing their core and shell sizes, it is possible to tailor the electron and hole wavefunctions overlap and tune CdSe/CdS NRs from Type-I-like to quasi-Type-II-like band alignment, which can be an important design consideration when engineering the gain/loss mechanisms in practical lasing systems.¹⁹⁻²³ Moreover, due to the narrower band gap of CdS with respect to ZnS, the absorption cross-section of CdSe/CdS core/shell NRs is greatly enhanced.¹³

With all of these aforementioned promises, in the nanocrystal lasing context, CdSe/CdS NRs has become one of the most heavily studied material systems.^{18,24} Recently, single-mode, single-exciton and tunable laser emission on a silica microsphere²⁵ and low-threshold amplified spontaneous emission (ASE) and lasing with two-photon pumping mechanism¹⁰ have been successfully demonstrated with CdSe/CdS core/shell NRs. Moreover, it was shown that nearly temperature-independent ASE can be possible with CdSe/CdS core/shell NRs²⁶

and controllable transition of ASE peak from CdSe core region to CdS shell region can be finely tuned by changing the length of the nanorod and the excitation intensity.²¹ In addition, the tunability of electron and hole wavefunctions overlap in this material system has also been discussed in the literature for both entangled photon generation²⁷ and nanocrystal lasing applications.²⁰ However, to the best of our knowledge, controlled shifting of ASE peak with respect to the spontaneous emission in CdSe/CdS NRs through systematically changing the electronic property of the NRs has not been demonstrated. Here, as a result of the exciton-exciton interaction engineering via adjusting the core and the shell size, we show the electronic Type tunability of the NRs feature resulting in blue-shifting (Type-II-like); and red-shifting (Type-I-like) ASE with respect to the spontaneous emission of NRs pumped with two-photon absorption (TPA) optical pumping mechanism. We also verify the Type attributions of different size NRs by carefully studying their time-resolved decay dynamics, where transition from Type-I to Type-II-like behavior has indicated longer decay lifetimes as a consequence of the decreased electron and hole wavefunctions overlap, and hence, a smaller oscillator strength.

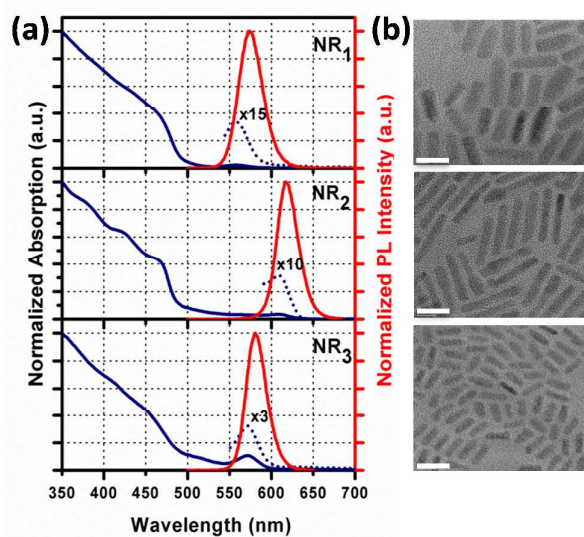


Figure 1. (a) Absorption and photoluminescence spectra of CdSe/CdS core/shell NRs with varied core sizes and rod lengths and (b) their high resolution transmission electron microscopy (TEM) images (scale bars = 10 nm).

In this study, we synthesized highly efficient and stable core-seeded CdSe/CdS NRs having different core sizes and rod lengths according to the recipe from the literature.¹⁵ As it can be seen from the TEM images (**Figure 1**), they exhibit highly crystalline structure with a narrow size distribution, which results in higher photoluminescence quantum efficiency (>40%). Owing to very small lattice mismatch between CdSe and CdS (3.9%), epitaxial growth of CdS shell is achieved. Therefore, it is not easy to differentiate CdSe and CdS regions and confirm the growth of CdS rod region without using strain analysis from the TEM images. However, the formation of CdS rod on top of CdSe core can be confirmed easily from the sharp increase in the absorption spectrum around 400-500 nm region (Figure 1), which corresponds to the band gap of wurtzite CdS. In addition, with the increase in rod length, this signature of rod region on absorption becomes more dominant and makes a significant contribution to the absorption cross-section. Thanks to this very high absorption of mainly rod-shaped shell

region of NRs, they are very good two-photon sensitizers, which is highly desirable for optical gain materials.¹³

For the optical gain study, all three high quality close-packed films were prepared by drop casting of highly concentrated solutions (100 mg/mL) of CdSe/CdS core/shell NRs on bare quartz substrates. The films were pumped with 120 fs laser pulses with 1 kHz repetition rate at the wavelength of 800 nm and the laser beam was focused on samples by using a cylindrical lens. The excitation intensity dependent emission spectrum of CdSe/CdS core/shell NR₂ sample having a core diameter of 3.8-4.0 nm and a rod length of 30.0 nm was given in **Figure 2**. At low excitation intensities, only spontaneous emission was observed having a peak at 632 nm with a full-width-at-half-maximum (FWHM) of 34 nm. When the excitation intensity exceeds the threshold value (~ 7.5 mJ/cm²), slightly red-shifted (~ 1 nm) ASE peak emerged at 634 nm with a FWHM value of 7 nm, which is very low as would be expected from an ASE process.

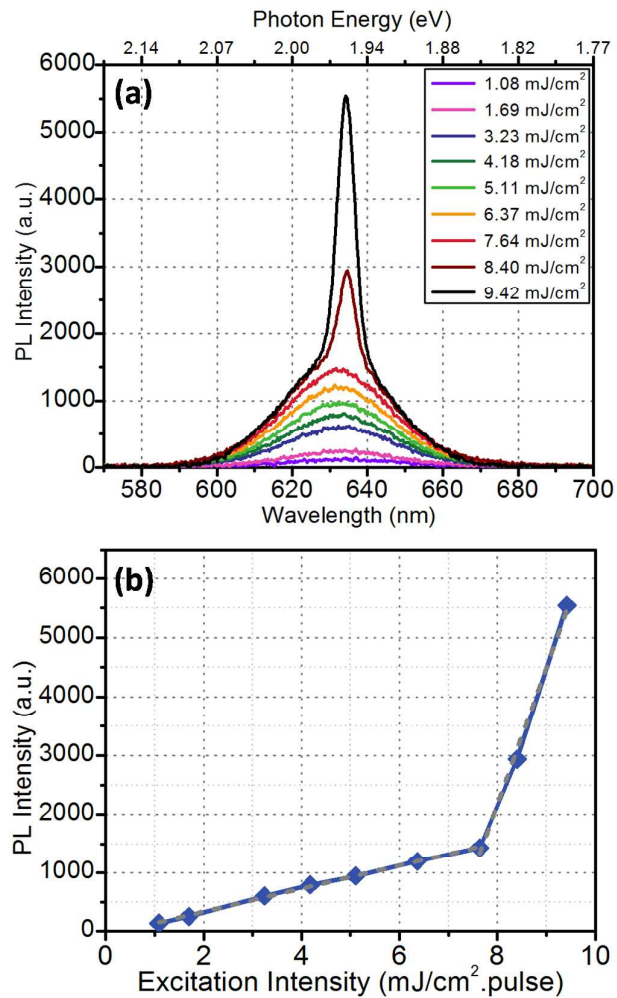


Figure 2. (a) Photoluminescence emission spectra of highly concentrated close-packed film of CdSe/CdS NR₂ sample under different excitation pulse intensities and (b) excitation pulse intensity dependence of the emission at the ASE peak position of CdSe/CdS NR₂.

In addition, it was shown that due to the lower energy barrier for electrons in CdSe/CdS core/shell material systems, type tunable electronic structure from Type-I to quasi Type-II was achieved by changing the core size and rod length.^{22,30} Therefore, in order to figure out the effect of different electronic structures on optical gain performance from the same material system, we designed and synthesized CdSe/CdS NRs with different core sizes and shell thicknesses. The films were prepared by drop-casting of highly concentrated solution of CdSe/CdS NRs on bare quartz substrates having no loss compensation or waveguiding

mechanism in order to make sure that the spectral position of the ASE peak is not affected by other parameters. We demonstrated type tunability of ASE peak originating from biexciton emission with respect to spontaneous emission via engineering attractive vs. repulsive nature of exciton-exciton interactions in the NRs. As a result of the smaller core size of NR₁, electrons were not confined to the CdSe core and a partial separation of electron and hole wavefunctions took place. Therefore, when we optically pumped the highly concentrated close-packed film of NR₁, we observed Type-II-like behavior with approximately 9 nm blue-shifted ASE peak due to repulsive exciton-exciton interaction (**Figure 3**).^{31,32} On the other hand, when the core size was increased as in the case of NR₃, the leakage of electrons to the CdS shell decreased, meaning that the core could confine most of the electrons; therefore, Type-I-like behavior was achieved with 4 nm red-shifted ASE peak from NR₃ owing to attractive exciton-exciton interaction. Finally, we observed that attractive vs. repulsive nature of exciton-exciton interaction can be modified not only by changing the core size but also the rod length. As it can be seen from Figure 3, slightly red-shifted (~1 nm) ASE peak was achieved from the NR₂ having a larger core size and a longer rod length, owing to the balanced attractive and repulsive exciton-exciton interaction. For this sample, looking at only the core size would suggest that the NRs should exhibit Type-I-like behavior and looking at the shell length would tell us that the NRs should behave like Type-II. However, with the balanced dominances of these two localization regimes, which resulted in neither attractive nor repulsive exciton-exciton interaction, we achieved non-shifted ASE peak.

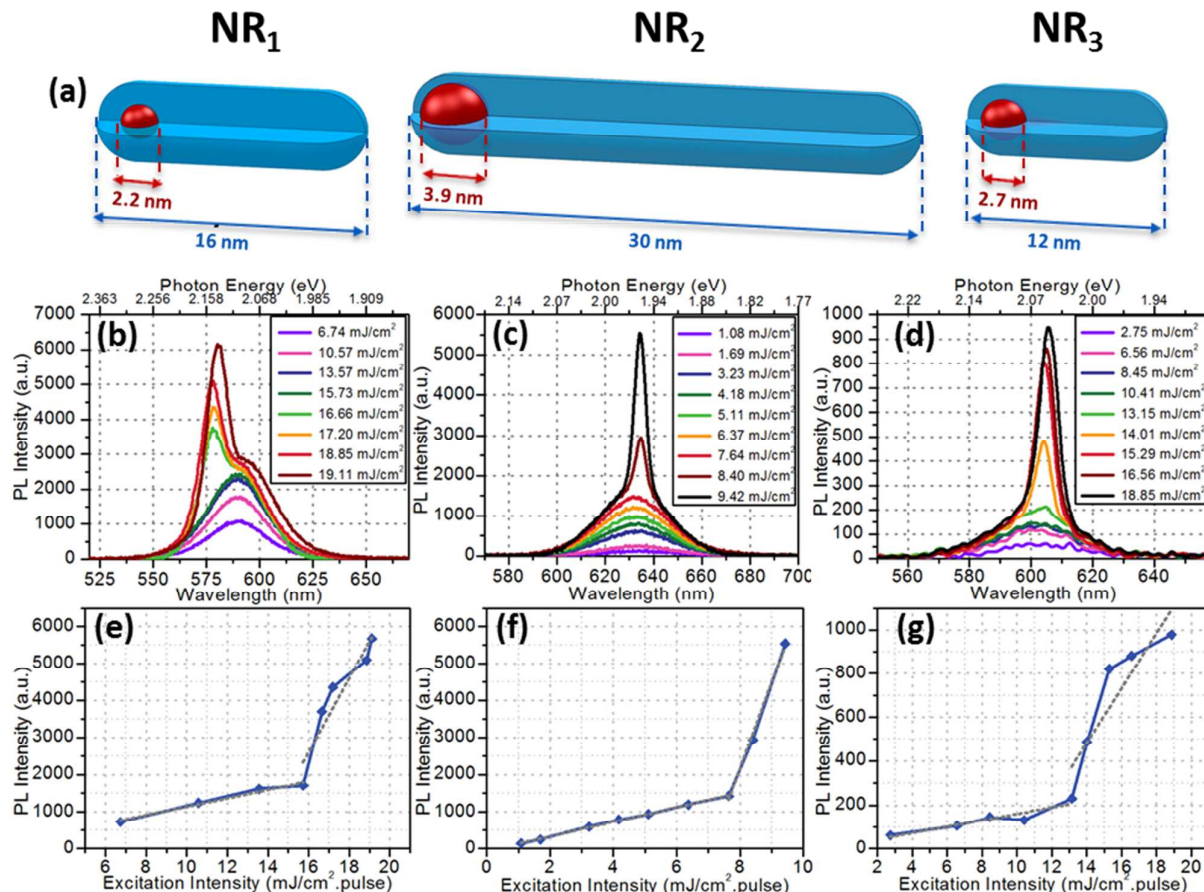


Figure 3. (a) Schematic illustration of CdSe/CdS core/shell NRs proportional to their size. (b), (c), (d) Excitation intensity dependent emission spectra of NR₁ (with blue-shifted ASE peak), NR₂ (with ASE peak at the same position as the spontaneous emission), and NR₃ (with red-shifted ASE peak), respectively. (e), (f), (g) Excitation pulse intensity dependences of emissions at the ASE peak positions of NR₁, NR₂, and NR₃, respectively.

In order to verify the hypothesis on electron and hole wavefunctions localization engineering stated above and gain more insight into the electronic band structure of CdSe/CdS core/shell NRs with different core sizes and rod lengths, we conducted time-resolved fluorescence measurements (TRF). We performed TRF measurements by using samples of NRs in solution with low concentrations under lower excitation intensities to assure that the NRs are occupied

with at most single excitons and nonradiative components are suppressed. TRF decay curves of CdSe/CdS NRs are given in **Figure 4**, and all of the decay curves exhibited almost single exponential decay. In literature, for the bare CdSe core nanocrystals, decreased radiative lifetime was demonstrated with decreased core size and, for the CdSe/CdS core/shell NRs, increased lifetime was reported with increasing the rod length.¹⁵ However, we observed the longest radiative lifetime (~ 30.2 ns) from the NR₁ sample having the smaller core size and shorter rod length, which also matches with the observed Type-II-like behavior from the blue-shifted ASE behavior.³³ In other words, owing to the smaller core size in NR₁, electrons were delocalized over the CdS shell region and with the decreased wavefunctions overlap of the electron and the hole, a longer radiative lifetime was observed (Figure 4). On the other hand, with the increased core size, leakage of electrons to the shell region was reduced and shorter radiative lifetimes was measured from the NR₃ as a result of increased electron and hole wavefunctions overlap, which can be explained by the Type-I-like behavior.

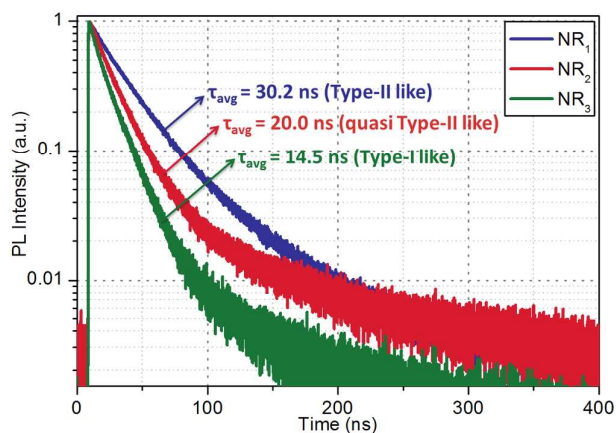


Figure 4. TRF decay curves of the NRs together with average least chi-square fitting lifetimes.

In order to perform a more detailed analysis on the tunability of ASE peak, we also synthesized CdSe/CdS core/shell NRs having different rod lengths while the size of cores and the diameter of rods are kept the same. The size of cores and the diameter of rods are 3.9-4.1 nm and 5.0-6.5 nm, respectively (**Figure S2**). **Figure 5** shows the photoluminescence spectra

of CdSe/CdS core/shell NRs having rod lengths of 22, 35 and 55 nm under intense two-photon optical pumping. In the case of NR₄ having a shorter rod length, we achieved ~1 nm red-shifted ASE peak with a FWHM value of 7 nm, which is expected due to their larger core size and shorter rod length (**Figure S3**). On the other hand, 8 nm blue-shifted ASE is observed for the case of NR₅ having a longer rod, which can be explained with the decreased electron and hole wavefunctions overlap as a result of the longer CdS rod region. This type-II-like ASE behavior of NR₅ is also verified by using TRF measurements. As a result of the delocalization of electrons, a longer radiative lifetime (23.0 ns) is observed from NR₅ while decreased radiative lifetime (16.4 ns) is observed from NR₄ (**Figure S4**). In addition, although NR₆ have the longest CdS rod length, we achieved almost the same amount (~8 nm) of blue-shifted ASE from NR₆ when compared to NR₅. It is also shown that both NR₅ and NR₆ have the same radiative lifetime, which confirms that photoluminescence lifetimes are a good indicator of confinement. Finally, optical gain thresholds down to 3 mJ/cm² are achieved from red-emitting CdSe/CdS core/shell NRs. When compared to the previous works of Jasieniak et al. (7 mJ/cm² threshold for red-emitting CdSe/CdS/ZnS CQDs employing a waveguiding mechanism)²⁸ and Todescato et al. (12.31 mJ/cm² threshold for red-emitting CdSe/CdZnS/ZnS CQDs with a waveguiding mechanism)²⁹, the optical gain threshold value can be said to be very low, which is attributed to the increased absorption cross-section.

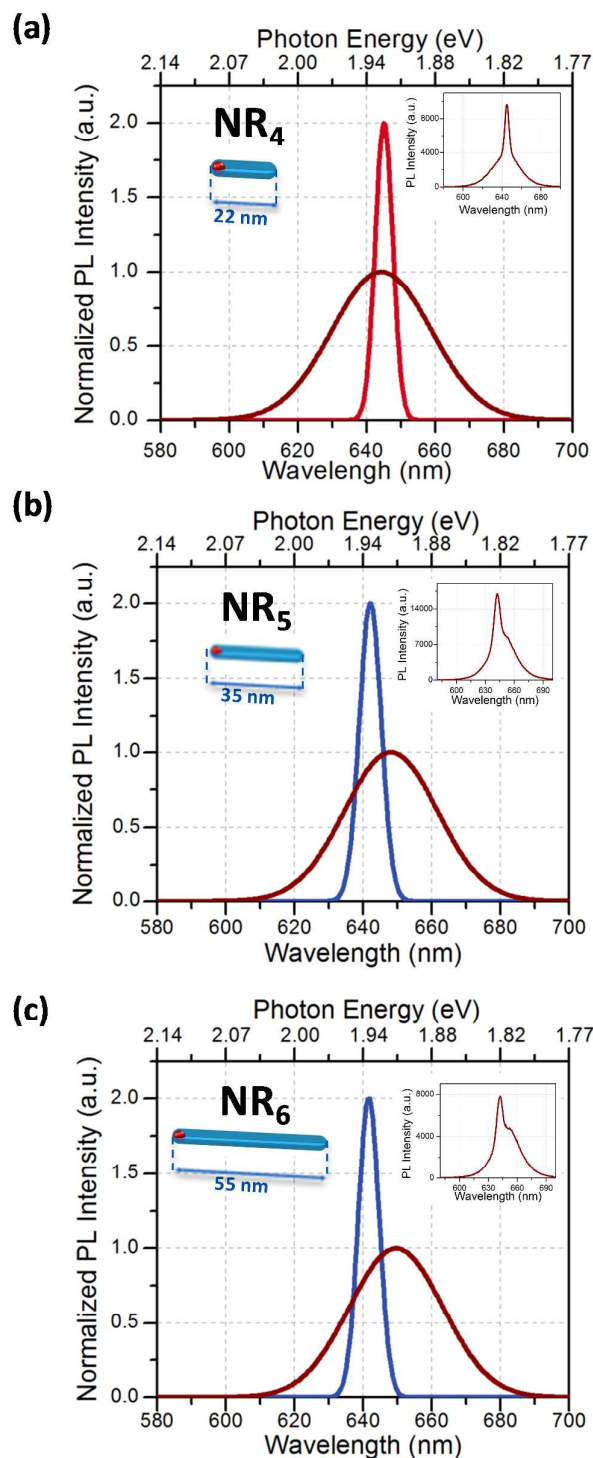


Figure 5. Normalized decomposed ASE and spontaneous emission spectra of (a) NR₄, (b) NR₅ and (c) NR₆ sample under intense two-photon optical pumping. The broad spectra (normalized to unity) are the spontaneous emission spectra of the NRs, while the narrow spectra are the ASE spectra of the NRs. The experimental PL spectra of NRs without decomposition are demonstrated in the inset.

Conclusion

In conclusion, we showed that with their giant two-photon absorption coefficients, CdSe/CdS NRs are one of the strongest candidates for lasing applications with two-photon optical pumping. Moreover, owing to their type tunable electronic configuration, blue-shifted and red-shifted ASE peak with respect to spontaneous emission was achieved via engineering the exciton-exciton interaction in the CdSe/CdS core/shell material system, which could prove useful when maximizing their optical gain performance, for example, through reducing reabsorption processes. Furthermore, we verified the type tunability of CdSe/CdS NRs with TRF measurements. These results show that with high two-photon absorption coefficient and ability to control ASE peak shift, CdSe/CdS NRs are very promising candidates for practical lasing applications.

Experimental Section

Synthesis of CdSe/CdS core/shell Nanorods

CdSe/CdS core/shell NRs are synthesized with seeded growth approach by using the slightly modified recipe from the literature.¹⁵ First, we synthesized CdSe cores. For a typical CdSe core synthesis, 3.0g of Trioctylphosphine oxide (TOPO), 0.280g of Octadecylphosphonic acid (ODPA) and 0.060g of Cadmium oxide (CdO) are loaded to the three-neck flask. The solution is evacuated at 150°C for an hour to remove oxygen and water inside the reaction solution. Then, the solution is heated to 350°C under argon atmosphere for the dissolution CdO. After the complete dissolution of CdO, 2mL of Trioctylphosphine (TOP) is injected swiftly. When the temperature is recovered to injection temperature of 350°C, selenium (Se) stock solution (0.058g Se and 0.5mL TOP) is injected. Different size of CdSe cores can be achieved by changing the growth time and the reaction is stopped by decreasing the temperature. Finally, CdSe cores are precipitated with ethanol and dissolved in toluene.

For the growth of CdS rod, 3g of TOPO, 0.290g of ODPA, 0.080g of hexylphosphonic acid (HPA) and 0.060g of CdO are loaded to the three-neck flask and evacuated at 150°C for an

hour. After evacuation, the temperature is increased to 350°C for the dissolution of CdO under the argon atmosphere. When the solution becomes colorless, 2mL of TOP is injected swiftly. After the temperature is recovered to 350°C, injection solution is injected and solution is kept at 350°C for the growth between 5-8 min. For the preparation of injection solution, certain amounts of CdSe core are precipitated. Then, these CdSe cores are dissolved freshly prepared sulfur (s) stock solution (0.200g S and 2mL TOP) inside the glove box. The reaction is stopped by decreasing the temperature and CdSe/CdS core/shell NRs are purified several times before optical gain studies by using ethanol. In addition, according to the desired rod length, the amounts of CdSe core, CdO and S can be tuned.

Measurement of the ASE spectra:

For the ASE experiments, as the excitation source for the NR samples, Spectra Physics, Spitfire Pro XP regenerative amplifier having 120 fs pulse width at 800 nm with a 1 KHz repetition rate is used. The amplifier is seeded by a Ti:Sapphire laser (Spectra Physics, Tsunami). The laser beam is focused on the sample with the help of a cylindrical lens having a 20 cm focal length and the samples are excited with a stripe geometry. A variable neutral density filter is used to adjust the pump intensity on the samples. The emission spectra of the samples were collected by an optical fiber connected to a miniature spectrometer (Maya2000 Pro).

Acknowledgements

This work is supported in part by the Singapore National Research Foundation under the program numbers of NRFCRP-6-2010-02 and NRF-RF-2009-09, and in part by ESF EURYL. Also, H.V.D. gratefully acknowledges support from TUBA-GEBIP. A.F.C. and Y.K. acknowledge support from TUBITAK BIDEB.

Notes and references

‡ These authors have contributed equally.

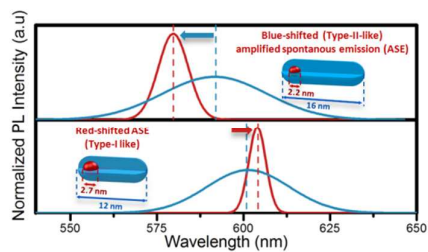
§ Present Address: Department of Electrical Engineering, Stanford University, Stanford, CA 94305, United States.

- 1 V. I. Klimov, A. A. Mikhailovsky, S. Xu, A. Malko, J. A. Hollingsworth, C. A. Leatherdale, H. -J. Eisler, M. G. Bawendi, *Science*, 2000, **290**, 314-317.
- 2 C. Dang, J. Lee, C. Breen, J. S. Steckel, S. Coe-Sullivan, *Nat. Nanotechnol.*, 2012, **7**, 335-339.
- 3 C. B. Murray, D. J. Norris, M. G. Bawendi, *J. Am. Chem. Soc.*, 1993, **115**, 8706-8715.
- 4 M. Kazes, D. Y. Lewis, Y. Ebenstein, T. Mokari, U. Banin, *Adv. Mater.*, 2002, **14**, 317-321.
- 5 A. V. Malko, A. A. Mikhailovsky, M. A. Petruska, J. A. Hollingsworth, H. Htoon, M. G. Bawendi, V. I. Klimov, *Appl. Phys. Lett.*, 2002, **81**, 1303-1305.
- 6 X. Peng, M. C. Schlamp, A. V. Kadavanich, A. P. Alivisatos, *J. Am. Chem. Soc.*, 1997, **119**, 7019-7029.
- 7 V. I. Klimov, J. A. McGuire, R. D. Schaller, V. I. Rupasov, *Phys. Rev. B*, 2008, **77**, 195324-12.
- 8 B. Fisher, J. M. Caruge, Y. T. Chan, J. Halpert, M. G. Bawendi, *Chem. Phys.*, 2005, **318**, 71-81.
- 9 J. M. Caruge, Y. Chan, V. Sundar, H. J. Eisler, M. G. Bawendi, *Phys. Rev. B*, 2004, **70**, 085316-7.
- 10 G. Xing, Y. Liao, X. Wu, S. Chakraborty, X. Liu, E. K. L. Yeow, Y. Chan, T. C. Sum, *ACS Nano*, 2012, **6**, 10835-10844.
- 11 M. Zavelani-Rossi, M. G. Lupo, F. Tassone, L. Manna, G. Lanzani, *Nano Lett.*, 2010, **10**, 3142-3150.
- 12 H. Htoon, J. A. Hollingsworth, A. V. Malko, R. Dickerson, V. I. Klimov, *Appl. Phys. Lett.*, 2003, **82**, 4776-4778.
- 13 G. Xing, S. Chakraborty, K. L. Chou, N. Mishra, C. H. A. Huan, Y. Chan, T. C. Sum, *Appl. Phys. Lett.*, 2010, **97**, 061112-3.
- 14 M. Zavelani-Rossi, M. G. Lupo, R. Krahné, L. Manna, G. Lanzani, *Nanoscale*, 2010, **2**, 931-935.
- 15 L. Carbone, C. Nobile, M. De Giorgi, F. D. Sala, G. Morello, P. Pompa, M. Hytch, E. Snoeck, A. Fiore, I. R. Franchini, M. Nadasan, A. F. Silvestre, L. Chiodo, S. Kudera, R. Cingolani, R. Krahné, L. Manna, *Nano Lett.*, 2007, **7**, 2942-2950.

- 16 D. V. Talapin, R. Koeppe, S. Götzinger, A. Kornowski, J. M. Lupton, A. L. Rogach, O. Benson, J. Feldmann, H. Weller, *Nano Lett.*, 2003, **3**, 1677-1681.
- 17 F. García-Santamaría, S. Brovelli, R. Viswanatha, J. A. Hollingsworth, H. Htoon, S. A. Crooker, V. I. Klimov, *Nano Lett.*, 2011, **11**, 687-693.
- 18 F. García-Santamaría, Y. Chen, J. Vela, R. D. Schaller, J. A. Hollingsworth, V. I. Klimov, *Nano Lett.*, 2009, **9**, 3482-3488.
- 19 A. F. Cihan, P. L. H. Martinez, Y. Kelestemur, E. Mutlugun, H. V. Demir, *ACS Nano*, 2013, **7**, 4799-4809.
- 20 M. Saba, S. Minniberger, F. Quochi, J. Roither, M. Marceddu, A. Gocalinska, M. V. Kovalenko, D. V. Talapin, W. Heiss, A. Mura, G. Bongiovanni, *Adv. Mater.*, 2009, **21**, 4942-4946.
- 21 R. Krahne, M. Zavelani-Rossi, M. G. Lupo, L. Manna, G. Lanzani, *Appl. Phys. Lett.*, 2011, **98**, 063105-3.
- 22 A. Sitt, F. D. Sala, G. Menagen, U. Banin, *Nano Lett.*, 2009, **9**, 3470-3476.
- 23 A. F. Cihan, Y. Kelestemur, B. Guzelturk, O. Yerli, U. Kurum, H. G. Yaglioglu, A. Elmali, H. V. Demir, *J. Phys. Chem. Lett.*, 2013, **4**, 4146-4152.
- 24 Y. Liao, G. Xing, N. Mishra, T. C. Sum, Y. Chan, *Adv. Mater.*, 2012, **24**, OP159-164.
- 25 C. Grivas, C. Li, P. Andreakou, P. Wang, M. Ding, G. Brambilla, L. Manna, P. Lagoudakis, *Nat. Commun.*, 2013, **4**, 1-9.
- 26 I. Moreels, G. Rainò, R. Gomes, Z. Hens, T. Stöferle, R. F. Mahrt, *Adv. Mater.*, 2012, **24**, OP231-235.
- 27 G. Rainò, T. Stöferle, I. Moreels, R. Gomes, Z. Hens, R. F. Mahrt, *ACS Nano*, 2012, **6**, 1979-1987.
- 28 J. J. Jasieniak, I. Fortunati, S. Gardin, R. Signorini, R. Bozio, A. Martucci, P. Mulvaney, *Adv. Mater.*, 2008, **20**, 69-73.
- 29 F. Todescato, I. Fortunati, S. Gardin, E. Garbin, E. Collini, R. Bozio, J. J. Jasieniak, G. D. Giustina, G. Brusatin, S. Toffanin, R. Signorini, *Adv. Funct. Mater.*, 2012, **22**, 337-344.
- 30 J. Müller, J. M. Lupton, P. G. Lagoudakis, F. Schindler, R. Koeppe, A. L. Rogach, J. Feldmann, D. V. Talapin, H. Weller, *Nano Lett.*, 2005, **5**, 2044-2049.
- 31 V. I. Klimov, S. A. Ivanov, J. Nanda, M. Achermann, I. Bezel, J. A. McGuire, A. Piryatinski, *Nature*, 2007, **447**, 441-446.
- 32 J. Nanda, S. A. Ivanov, M. Achermann, I. Bezel, A. Piryatinski, V. I. Klimov, *J. Phys. Chem. C*, 2007, **111**, 15382-15390.

- 33 G. Rainò, T. Stöferle, I. Moreels, R. Gomes, J. S. Kamal, Z. Hens, R. F. Mahrt, *ACS Nano*, 2011, **5**, 4031-4036.

Table of Content Figure



Controlling the exciton-exciton interaction by varying the core and shell size, blue-shifted and red-shifted amplified spontaneous emission are systematically demonstrated.